

Article

ZnO@TiO₂ Core/Shell Nanowire Arrays with Different Thickness of TiO₂ Shell for Dye-Sensitized Solar Cells

Liqing Liu ¹, Hui Wang ¹, Dehao Wang ², Yongtao Li ¹, Xuemin He ¹, Hongguang Zhang ¹ and Jianping Shen ^{2,*}

¹ New Energy Technology Engineering Laboratory of Jiangsu Province & School of Science, Nanjing University of Posts and Telecommunications (NJUPT), Nanjing 210023, China; liulq@njupt.edu.cn (L.L.); B16011501@njupt.edu.cn (H.W.); liyt@njupt.edu.cn (Y.L.); hxm@njupt.edu.cn (X.H.); Zhanghongguang2003@126.com (H.Z.)

² College of Electronic and Optical Engineering, Nanjing University of Post and Telecommunications, Nanjing 210023, China; 1218022814@njupt.edu.cn

* Correspondence: jianpingshen@njupt.edu.cn

Received: 9 March 2020; Accepted: 15 April 2020; Published: 21 April 2020



Abstract: The ZnO@TiO₂ core/shell nanowire arrays with different thicknesses of the TiO₂ shell were synthesized, through depositing TiO₂ on the ZnO nanowire arrays using the pulsed laser deposition process. Scanning electron microscopy (SEM) and transmission electron microscopy (TEM) images show that these core/shell nanowires were homogeneously coated with TiO₂ nanoparticles with high crystallinity, appearing to be a rather rough surface compared to pure ZnO nanowires. The efficiency of ZnO@TiO₂ core/shell structure-based dye-sensitized solar cells (DSSCs) was improved compared with pure ZnO nanowires. This is mainly attributed to the enlarged internal surface area of the core/shell structures, which increases dye adsorption on the anode to improve the light harvest. In addition, the energy barrier which formed at the interface between ZnO and TiO₂ promoted the charge separation and suppressed the carrier recombination. Furthermore, the efficiency of DSSCs was further improved by increasing the thickness of the TiO₂ shell. This work shows an efficient method to achieve high power conversion efficiency in core/shell nanowire-based DSSCs.

Keywords: ZnO@TiO₂ nanowire arrays; dye-sensitized solar cells; pulsed laser deposition method; different thickness shell

1. Introduction

With the development of global industry, energy demand is rapidly increasing, while the traditional fossil fuels are estimated to be depleted in a few decades. The environmental problems caused by fossil fuels are also getting serious. Therefore, the development of new clean energy is imperative. The large-scale photovoltaic cell is the most promising avenue to solve the energy shortage issue, as it can convert the clean and unexhausted solar radiation to electric energy. Dye-sensitized solar cells (DSSCs) are regarded as the most promising photovoltaic device with the advantages of being flexible, inexpensive and easier to fabricate [1,2]. As the main component of DSSCs, the photosensitized anode typically consists of porous semiconductor nanoparticle films (such as TiO₂), with a typical film thickness of 10 μm and a nanoparticle size of 10~30 nm in diameter [2]. These nanoparticle films have a large internal surface area for the absorption of dye molecules to increase the light harvest. However, grain boundaries of the nanoparticles cause the electron scatter or act as the electron trap to dramatically decrease the electron diffusion [3]. The diffusion coefficient in the mesoporous network is several orders of magnitude lower than that of anatase single crystalline TiO₂ (~0.4 cm² s⁻¹) [4].

Reported mobility values in this regime vary between 0.01 and 0.05 cm² V s⁻¹ [5,6]. This shortage becomes more serious when the thickness of photoelectrode film is increased, which results in the limitation of the electron diffusion length in the nanoparticle anode to 10–15 μm [7]. The further improvement of the power conversion efficiency is retarded because the effective thickness of the anode films cannot be increased.

One-dimensional (1-D) nanostructures can effectively eliminate the shortage mentioned above, because the grain boundaries effect could be restricted [8,9]. Moreover, 1-D nanostructures, such as aligned vertically nanowire or nanotube arrays, could provide short electron transmission pathways which ensure the rapid collection of photo-generated carriers throughout the device [10–12]. ZnO owns higher electron mobility than that of TiO₂, by 2–3 orders of magnitude. It is reported that the electron mobility of ZnO bulk material is 200–300 cm² V s⁻¹ and ZnO single-crystal nanowires is ~1000 cm² V s⁻¹ [13–15], respectively. Therefore, 1-D ZnO nanowire is considered as one of the most promising materials in solar cells, for fast electron transport with reduced recombination. It's found that the electron diffusion length increased in ordered 1-D ZnO nanowire arrays on the order of 100 μm [16,17]. So, the energy conversion efficiency can be improved by increasing the thickness of the sensitized films. However, the key challenge of using vertically aligned 1-D nanostructure in DSSCs is the low internal surface area comparison with mesoporous nanoparticle films, which results in less dye adsorption and therefore low light-harvesting efficiency [18–20]. Long nanowires arrays are desired to achieve the same efficiency as the mesoporous films. For example, Xu CK et al. [21] assembled four layers of ZnO nanowire arrays with thickness of up to 40 μm, for using as an anode of DSSCs, with power conversion efficiencies of up to 7%. However, the growth of long nanowires is commonly time consuming [12]. So, this is an effective method to deposit a shell on these 1-D nanostructures, to increase the surface roughness. The shell is also considered to be a blocking layer for suppressing the electron-hole pair recombination by forming an energy barrier on the interface of ZnO@TiO₂ [22,23]. Many novel core/shell structures, including ZnO@TiO₂ [24], ZnO@In₂S₃ [25,26], ZnO@CdSe [27] and so forth, have been achieved. The conversion efficiencies of such core/shell structures have been improved. Therefore, surface modification contributes to high performance DSSCs. However, it is still a challenge to control the thickness, size, crystallinity and homogeneity of the shell to optimize the anode in DSSCs.

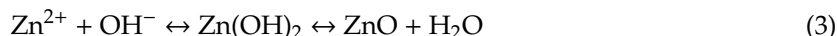
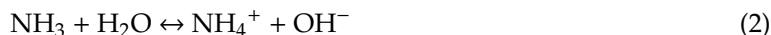
In this paper, the ZnO@TiO₂ core/shell structures are synthesized using two steps. Firstly, the vertical ZnO nanowires were fabricated by microwave heating method. Secondly, the TiO₂ shell was deposited on the surface of ZnO nanowires by pulsed laser deposition (PLD) process. By adjusting the pulsed number, the ZnO@TiO₂ core/shell structures with different thickness shells have been obtained. It indicates that the TiO₂ particles were coated uniformly on the surface of the ZnO nanowires. The performance of the ZnO@TiO₂ composited nanowire arrays based DSSCs was examined under a solar simulator. Current density–voltage (*J*-*V*) curves show that the power conversion efficiency increases with the thickness of the shell layer. This result indicates that this composited structure can enlarge the internal surface area and consequently increase the light harvest.

2. Experimental Section

2.1. Preparation of Well Aligned ZnO Nanowire Arrays

The well aligned ZnO nanowire arrays were fabricated using the microwave-assisted hydrothermal method on fluorine doped tin oxide (FTO) glass substrate, similar to our previous report [28]. Furthermore, 12.5 mM zinc nitrate hexahydrate (Zn(NO₃)₂·6H₂O, 99.99%, product number: Z111706) and 25 mM hexamethylenetetramine (HMTA, C₆H₁₂N₄, ≥99.0%, product number: H116380) were mixed to grow ZnO nanowire arrays. Then, the substrate with ZnO seeds was suspended vertically in the beaker with the mixture aqueous solution heated by microwave oven for 2 h. After reaction, the substrate was taken out and rinsed softly several times, using deionized (DI) water and dried in

air flow (all chemicals in this work were purchased from Aladdin, Shanghai, China). Additionally, ZnO nanowires are synthesized based on the following reaction:



2.2. Preparation of TiO₂ Shell

TiO₂ nanoparticles were deposited on ZnO nanowires by PLD process, with different pulse numbers of 1000, 3000, and 5000 respectively (schematic drawing was shown in Figure 1). The FTO substrates with ZnO nanowire arrays and the TiO₂ target were transferred into the PLD chamber. The preparation condition is similar to our previous work [29], the pressure of the chamber was $\sim 6 \times 10^{-4}$ Pa, the high purity oxygen gas pressure was ~ 5 Pa, the pulse energy was 450 mJ, and the temperature in the chamber was 450 °C. After deposition, the samples were annealed at 450 °C in situ for 30 min under the oxygen gas pressure of 4×10^{-3} Pa, for reducing defect and improving crystalline. The crystallization and thickness of TiO₂ shells could be controlled by tuning the experimental parameters, such as pulse number, energy, temperature and the distance between substrate and target.

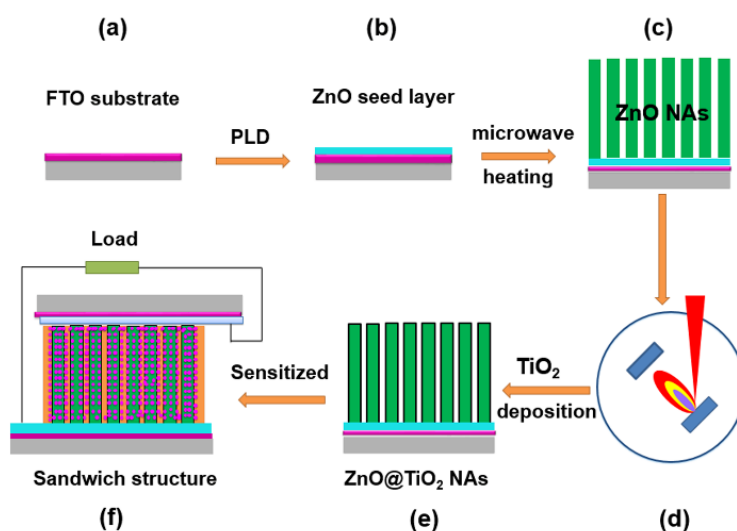


Figure 1. Schematic drawing of the synthesis process of the samples. (a) FTO glass substrate; (b) ZnO seed layer; (c) ZnO nanowire arrays; (d) TiO₂ shell is deposited on ZnO surface by PLD; (e) ZnO@TiO₂ nanowire arrays; (f) sandwich structure of solar cell.

2.3. Fabrication of DSSCs

The area of the ZnO@TiO₂ core/shell nanostructures is 0.5 cm². The ZnO@TiO₂ core/shell structures were first sintered at 450 °C for 1 h, to eliminate any residual organics and moisture. After sintering, the samples were left to cool to 100 °C and then immediately immersed in an ethanol solution of 0.5 mM (Bu₄N)₂[Ru(4,4'-(COOH)-2,2'-bipyridine)₂(NCS)₂] (N719 dye, 90%, product number: B132959) for 12 h [30]. The samples were withdrawn from the solution, rinsed in acetonitrile, and dried in air. The platinum film coated on the FTO glass substrate was used for counter electrode and then the sandwiched structure was assembled. The distance between the two electrodes is 50 μm. The electrolytic solution consisted of 0.1 M LiI (99.995%, product number: L118835), 0.1 M I₂ (product number: I298615), 0.5 M tert-butylpyridine (96%, product number: B109674) and 0.6 M tetrabutylammonium iodide ($\geq 99.0\%$, product number: T103716) in acetonitrile. It was introduced into the gap formed by the

two electrodes by capillary force. The performance of the DSSCs was measured under AM 1.5 G (100 mW/cm^2) simulated sunlight.

3. Characterizations

The morphologies of the samples were observed by field emission scanning electron microscopy (FESEM, FEI Inspect F50, USA). The crystal structures of ZnO@TiO₂ core/shell nanowire arrays were studied by X-ray diffraction (XRD, Rigaku Smartlab, Japan) with Cu-K α radiation ($\lambda = 0.15406 \text{ nm}$). Transmission electron microscope (TEM) images were carried out by a Tecnai G2 F20 TEM (FEI, USA). Energy-dispersive X-ray (EDX) spectroscopy was also conducted during the SEM experiments.

4. Results and Discussion

The XRD result is similar to our previous work (Figure 2) [29] and proves that all the diffraction peaks of ZnO can be indexed as being of the hexagonal wurtzite-type ZnO (JCPDS card No. 36-1451), with space group of $P6_3mc$. The diffraction peaks of TiO₂ can be indexed as of anatase TiO₂ with interplanar spacing of 0.35 nm, and the intensity of the typical peak is stronger with the thickness of the TiO₂ shell.

Figure 2a,b display the whole SEM images of the aligned ZnO nanowire arrays fabricated by microwave heating method on the FTO substrate. It's clear to see that these nanowires were not all grown perpendicularly to the substrate, and the diameter of the nanowires are not uniform; this is due to the fact that the surface of the FTO glass substrate is very rough, so the nucleation sites are not uniform, resulting in them not being vertically aligned and not being uniform of the growth nanowire arrays. The length of nanowires is $\sim 3.5 \mu\text{m}$. In addition, the top of the nanowires is a little tapered, which is related to the rate of injection of fresh solution using our method. The faster the chemical reaction (the faster the rate), the sharper the top of the nanowires. From Figure 2a, it is evident that there is enough space between these nanowires. This is not only beneficial to the deposition of the TiO₂ shell on the ZnO nanowires, but also helpful for the entrance of dye molecules. Figure 2b is the SEM image of pure ZnO nanowires with high magnification. It can be seen that the surfaces of the nanowires are rather smooth. The SEM images of nanowires coated with a layer of TiO₂ are shown in Figure 2c,d. Figure 2c displays the sample which is ZnO nanowire core deposited with a TiO₂ shell; the coated nanowires still maintained the nanowire morphology, as shown in Figure 2a, while the shape is changed slightly. In the SEM image with large magnification (Figure 2d), a lot of small nanoparticles are found to cover the core nanowires. The surfaces of the nanowires after coating become rough compared with pure ZnO nanowires (Figure 2b), indicating the successful coating of TiO₂ on the surface of ZnO nanowires, to form the ZnO@TiO₂ core/shell nanowires. Though the TiO₂ shell layer reduces the space between these nanowires, there is still enough space between these nanowires for electrolyte transformation. As for the thickness of the TiO₂ shell, we can change it by adjusting the number of the laser pulses. Figure 3a,b show the SEM images of the samples with TiO₂ shells of 1000 and 5000 pulses, respectively. Similar nanowires with rough surfaces, such as those shown in Figure 2, can be also observed. The different roughness of the surface is caused by the thickness of the TiO₂ shell layer.

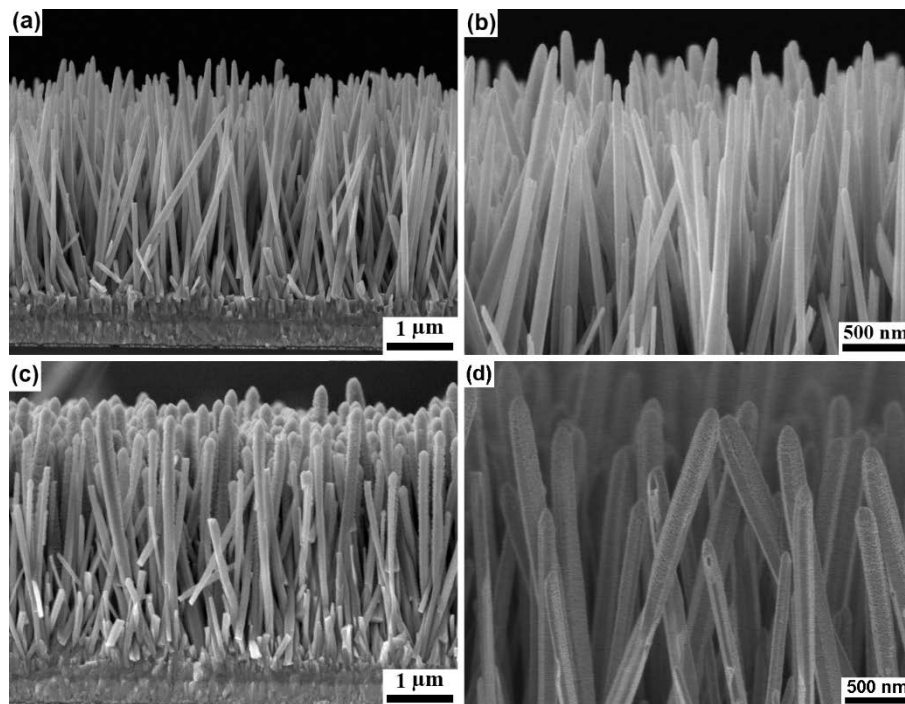


Figure 2. Cross-sectional SEM images of aligned ZnO nanowire arrays (a,b) and ZnO@TiO₂ core/shell nanowire arrays by microwave heating method followed by PLD process, depositing TiO₂ with 3000 pulses (c,d).

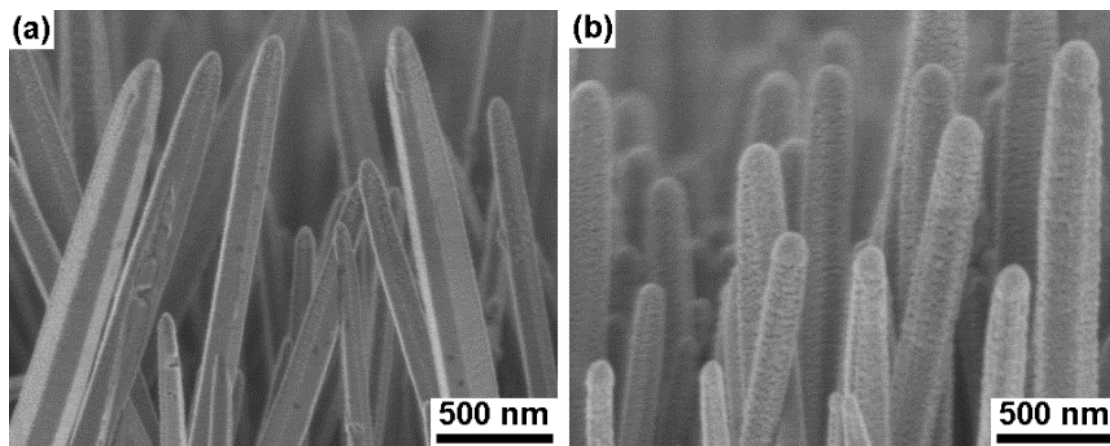


Figure 3. SEM of ZnO@TiO₂ core/shell nanowire arrays synthesized with 1000 pulses (a) and 5000 pulses (b), respectively.

Figure 4 displays the energy dispersive X-ray (EDX) spectra of synthesized pure ZnO (1#) and ZnO@TiO₂ core/shell nanowire arrays, with different pulse numbers of 1000 (2#), 3000 (3#) and 5000 (4#), respectively. These spectra indicate that the core/shell nanowires are composed of Zn, O and Ti elements only. The intensity of the peak corresponding to Ti element increases with the pulse number. The atomic ratio of the Ti element is about 2.7%, 8.0% and 11.8% for the sample of 2#, 3# and 4#, respectively. The inset (Figure 4) shows the atomic ratio of Ti as the function of pulse numbers. It is shown that the amount of Ti element is almost linearly increased with the number of the laser pulses. This suggests that the thickness of the TiO₂ shell can be well adjusted by changing the pulse number.

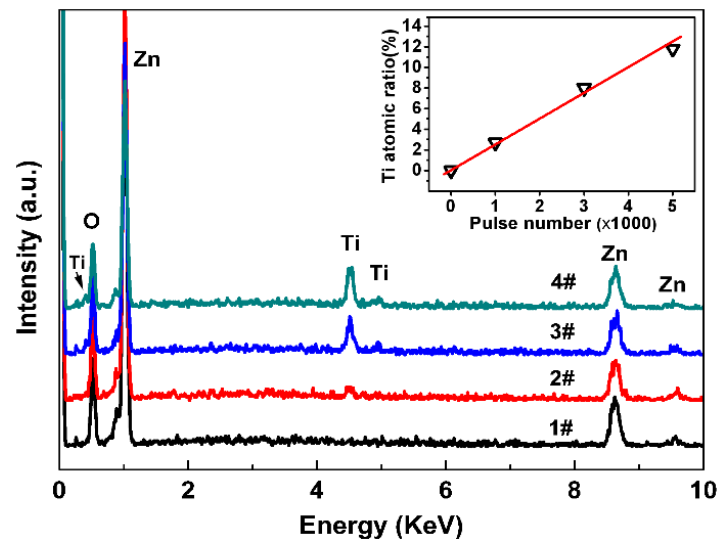


Figure 4. EDX spectra of ZnO (1#) and ZnO@TiO₂ core/shell nanowire arrays with different pulse number of 1000 (2#), 3000 (3#) and 5000 (4#). Inset shows the Ti atomic ratio as the function of pulse number.

The TEM images of an individual ZnO@TiO₂ core/shell nanowire are presented in Figure 5a,b. The small nanoparticles on the surface of the core nanowire are TiO₂. It can be clearly seen that the whole ZnO nanowire was rather homogeneously coated with TiO₂ shell. The average size of the TiO₂ nanoparticles is about 5 nm. Figure 5c shows the high-resolution (HR) TEM images of ZnO@TiO₂ core/shell nanowire, fabricated by PLD depositing TiO₂ layer on ZnO nanowire. From Figure 5c, the interface between ZnO and TiO₂ can be clearly identified. Figure 5d shows the enlarged HRTEM image of the interface region between the ZnO core and the TiO₂ shell. The lattice spacing of ZnO and TiO₂ shown in Figure 5d are 0.25 and 0.35 nm, which match the lattice spacing of (002) plane of ZnO and (101) plane of anatase TiO₂, respectively. The lattice fringes in the ZnO and shell layer of TiO₂ indicate that the ZnO@TiO₂ core/shell nanowire is well crystallized. Therefore, it's a useful method for synthesizing core/shell structures by the PLD process deposited shell layer on the core nanowire arrays.

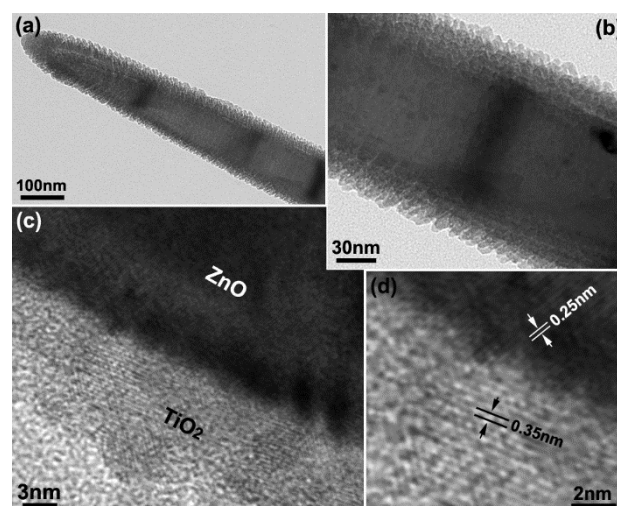


Figure 5. TEM (a,b) and HRTEM (c,d) images of ZnO@TiO₂ core/shell nanowire arrays fabricated by pulsed laser deposition (PLD) depositing TiO₂ layer on ZnO nanowire.

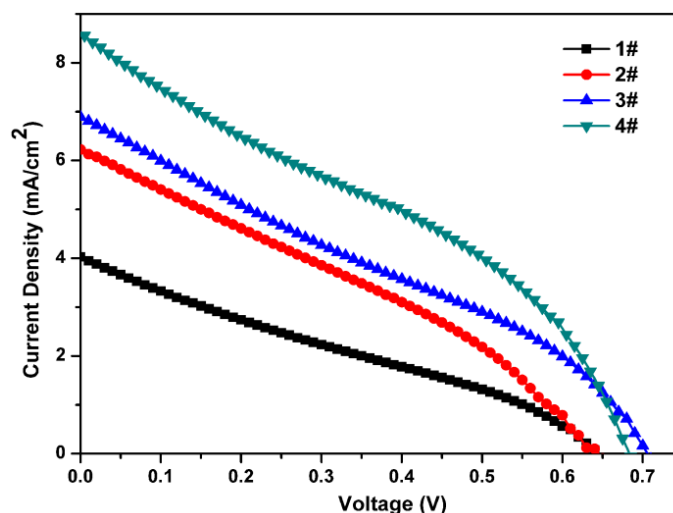


Figure 6. Photocurrent density-voltage curves of ZnO and ZnO@TiO₂ core/shell nanowire arrays, with different thicknesses of the TiO₂ shell.

Figure 6 shows the J - V characteristics of pure ZnO nanowire arrays (1#) and ZnO@TiO₂ core/shell structures with different thicknesses of TiO₂ shells (2#, 3# and 4#) based DSSCs. The open circuit voltage (V_{oc}), short circuit current density (J_{sc}), fill factor (FF) and power conversion efficiency (η) of pure ZnO and ZnO@TiO₂ nanowire arrays were listed in Table 1. As expected, the J_{sc} and η are increased with the increase of the TiO₂ shells' thickness. The FF is also increased, so that the η of 4# is almost three times higher than that of the pure ZnO nanowire arrays. This improvement is probably for several reasons. First, the internal surface area of the coated ZnO is enlarged for the fine nanoparticles on the surface of ZnO nanowires, promoting more dye to be adsorbed on the anode to increase the light harvest. From Figures 2 and 3, the surface of the nanowires, after being coated with a layer of TiO₂, becomes rough compared with pure ZnO nanowires, so that more dye is adsorbed on the surface to improve the power conversion efficiency. The efficiency of the ZnO@TiO₂ core/shell nanowire array-based DSSCs increases with the thickness of the TiO₂ shell increasing, which is mainly attributed to the larger surface area for the thicker TiO₂ shell and therefore increasing the dye-loading amount. Second, the TiO₂ barrier layer can improve the chemical stability of ZnO nanowire [31]. Third, the heterojunction which formed at the interface between ZnO and TiO₂ promoted the charge separation and suppressed the carrier recombination [32].

Table 1. The photovoltaic parameters of the dye-sensitized solar cells (DSSCs) based on the ZnO and ZnO@TiO₂ core/shell nanowire arrays, with different thicknesses of TiO₂ shell.

Samples	J_{sc} (mA/cm ²)	V_{oc} (V)	FF	η (%)
1#	4.03	0.64	0.27	0.71
2#	6.23	0.65	0.31	1.24
3#	6.89	0.71	0.30	1.46
4#	8.63	0.68	0.35	2.04

5. Conclusions

We successfully synthesized ZnO@TiO₂ core/shell nanowire arrays through depositing TiO₂ particles by PLD process on the ZnO nanowire arrays, fabricated by a controllable hydrothermal growth method. SEM and TEM images show that the anatase TiO₂ particles with high crystallinity were homogeneously coated on the vertical ZnO nanowires. By changing the pulse number during the PLD experiments, the thickness of TiO₂ shells can be adjusted. The efficiency of the ZnO@TiO₂ core/shell nanowire arrays based DSSCs increases with the thickness of the shell increasing. Because

the shells of TiO₂ were homogeneously deposited on the whole surface of the ZnO nanowires, the composited nanowires have an enlarged internal surface area to increase the amount of dye loading. So, the characteristics of the ZnO@TiO₂ core/shell nanowire arrays were greatly improved, compared with those of the pure ZnO nanowire. Moreover, the effects of shell thickness of the core/shell structures based DSSCs were investigated. It is found that the efficiency of DSSCs was further improved through increasing the thickness of TiO₂ shell, which is mainly attributed to the TiO₂ nanoparticles homogeneously coated on the whole ZnO nanowire. Therefore, the inner surface of the core/shell structures increases and dye-loading amount was enhanced. The heterojunction which formed at the interface between ZnO and TiO₂ promoted the charge separation and suppressed the carrier recombination. Because coating TiO₂ nanoparticles on ZnO nanowire can greatly increase the internal surface area to increase the light harvest, it can achieve the comparative high η in rather short 1-D nanostructure arrays. For the fast electron transportation and long electron diffusion length in 1-D nanostructure, 1-D core-shell nanowire is a promising structure to obtain DSSCs with high performance.

Author Contributions: Conceptualization, methodology, writing—original draft preparation, writing—review and editing, L.L.; investigation, H.W.; investigation, D.W.; formal analysis, writing—review and editing, Y.L., X.H. and H.Z.; project administration, J.S. All authors have read and agreed to the published version of the manuscript.

Funding: This research was funded by the National Natural Science Foundation of China (Grants No. 61874058, 51861145301), Nanjing University of Posts and Telecommunications under research projects (Grants No. NY220036, NY217096) and Nanjing University of Posts and Telecommunications Foundation under Grant JUH219002, Grant JUH219007.

Conflicts of Interest: The authors declare no conflict of interest.

References

1. Agarkar, S.A.; Dhas, V.V.; Muduli, S.; Ogale, S.B. Dye sensitized solar cell (DSSC) by a novel fully room temperature process: A solar paint for smart windows and flexible substrates. *RSC Adv.* **2012**, *2*, 11645–11649. [[CrossRef](#)]
2. O'Regan, B.; Gratzel, M. A low-cost, high-efficiency solar cell based on dye-sensitized colloidal TiO₂ films. *Nature* **1991**, *353*, 737–740. [[CrossRef](#)]
3. Thavasi, V.; Renugopalakrishnan, V.; Jose, R.; Ramakrishna, S. Controlled electron injection and transport at materials interfaces in dye sensitized solar cells. *Mater. Sci. Eng. R* **2009**, *63*, 81–99. [[CrossRef](#)]
4. Forro, L.; Chauvet, O.; Emin, D.; Zuppiroli, L.; Berger, H.; Lévy, F. High mobility n-type charge carriers in large single crystals of anatase (TiO₂). *J. Appl. Phys.* **1994**, *75*, 633–635. [[CrossRef](#)]
5. Greijer, A.H.; Boschloo, G.; Hagfeldt, A. Conductivity studies of nanostructured TiO₂ films permeated with electrolyte. *J. Phys. Chem. B* **2004**, *108*, 12388–12396. [[CrossRef](#)]
6. Van de Krol, R.; Goossens, A.; Meulenkamp, E.A. Electrical and optical properties of TiO₂ in accumulation and of lithium titanate Li_{0.5}TiO₂. *J. Appl. Phys.* **2001**, *90*, 2235–2242. [[CrossRef](#)]
7. Dai, S.Y.; Wang, K.J. Optimum nanoporous TiO₂ film and its application to dye-sensitized solar cell. *Chin. Phys. Lett.* **2003**, *20*, 953.
8. Xu, C.; Shin, P.H.; Cao, L.; Wu, J.; Gao, D. Ordered TiO₂ nanotube arrays on transparent conductive oxide for dye-sensitized solar cells. *Chem. Mater.* **2009**, *22*, 143–148. [[CrossRef](#)]
9. Yu, K.H.; Chen, J.H. Enhancing solar cell efficiencies through 1-D nanostructures. *Nanoscale Res. Lett.* **2009**, *4*, 1–10. [[CrossRef](#)]
10. Ajmal Khan, M.; Ishikawa, Y.; Kita, I.; Fukunaga, K.; Fuyukib, T.; Konagai, M. Control of verticality and (111) orientation of In-catalyzed silicon nanowires grown by the vapour-liquid-solid mode for nanoscale device applications. *J. Mater. Chem. C* **2015**, *3*, 11577–11580. [[CrossRef](#)]
11. Song, H.; Lee, K.H.; Jeong, H.; Um, S.H.; Han, G.S.; Jung, H.S.; Jung, G.Y. A simple self-assembly route to single crystalline SnO₂ nanorod growth by oriented attachment for dye sensitized solar cells. *Nanoscale* **2013**, *5*, 1188. [[CrossRef](#)] [[PubMed](#)]
12. Ajmal Khan, M.; Ishikawa, Y.; Kita, I.; Tani, A.; Yano, H.; Fuyuki, T.; Konagai, M. Investigation of crystallinity and planar defects in the Si nanowires grown by vapor-liquid-solid mode using indium catalyst for solar cell applications. *Jpn. J. Appl. Phys.* **2016**, *55*, 01AE03. [[CrossRef](#)]

13. Özgür, Ü.; Alivov, Y.I.; Liu, C.; Teke, A.; Reshchikov, M.A.; Doğan, S.; Avrutin, V.; Cho, S.J.; Morkoç, H. A comprehensive review of ZnO materials and devices. *J. Appl. Phys.* **2005**, *98*, 041301. [[CrossRef](#)]
14. Tang, H.; Prasad, K.; Sanjinès, R.; Schmid, P.E.; Lévy, F. Electrical and optical properties of TiO₂ anatase thin films. *J. Appl. Phys.* **1994**, *75*, 2042–2047. [[CrossRef](#)]
15. Bae, H.S.; Yoon, M.H.; Kim, J.H.; Im, S. Photodetecting properties of ZnO-based thin-film transistors. *Appl. Phys. Lett.* **2003**, *83*, 5313–5315. [[CrossRef](#)]
16. Martinson, A.B.F.; McGarrah, J.E.; Parpia, M.O.K.; Hupp, J.T. Dynamics of charge transport and recombination in ZnO nanorod array dye-sensitized solar cells. *Phys. Chem. Chem. Phys.* **2006**, *8*, 4655–4659. [[CrossRef](#)]
17. Jennings, J.R.; Ghicov, A.; Peter, L.M.; Schmuki, P.; Walker, A.B. Dye-sensitized solar cells based on oriented TiO₂ nanotube arrays: Transport, trapping, and transfer of electrons. *J. Am. Chem. Soc.* **2008**, *130*, 13364–13372. [[CrossRef](#)]
18. Mor, G.K.; Shankar, K.; Paulose, M.; Varghese, O.K.; Grimes, C.A. Use of highly-ordered TiO₂ nanotube arrays in dye-sensitized solar cells. *Nano Lett.* **2005**, *6*, 215–218. [[CrossRef](#)]
19. Feng, X.; Shankar, K.; Varghese, O.K.; Paulose, M.; Latempa, T.J.; Grimes, C.A. Vertically aligned single crystal TiO₂ nanowire arrays grown directly on transparent conducting oxide coated glass: Synthesis details and applications. *Nano Lett.* **2008**, *8*, 3781–3786. [[CrossRef](#)]
20. Liu, B.; Aydil, E.S. Growth of oriented single-crystalline rutile TiO₂ nanorods on transparent conducting substrates for dye-sensitized solar cells. *J. Am. Chem. Soc.* **2009**, *131*, 3985–3990. [[CrossRef](#)]
21. Xu, C.; Wu, J.; Desai, U.V.; Gao, D. Multilayer assembly of nanowire arrays for dye-sensitized solar cells. *J. Am. Chem. Soc.* **2011**, *133*, 8122–8125. [[CrossRef](#)] [[PubMed](#)]
22. Abd-Ellah, M.; Moghimi, N.; Zhang, L.; Thomas, J.P.; McGillivray, D.; Srivastava, S.; Leung, K.T. Plasmonic gold nanoparticles for ZnO-nanotube photoanodes in dye-sensitized solar cell application. *Nanoscale* **2016**, *8*, 1658–1664. [[CrossRef](#)] [[PubMed](#)]
23. Hernandez, S.; Cauda, V.; Chiodoni, A.; Dallorto, S.; Sacco, A.; Hidalgo, D.; Celasco, E.; Pirri, C.F. Optimization of 1D ZnO@TiO₂ core-shell nanostructures for enhanced photoelectrochemical water splitting under solar light illumination. *ACS Appl. Mater. Interfaces* **2014**, *6*, 12153–12167. [[CrossRef](#)] [[PubMed](#)]
24. Law, M.; Greene, L.E.; Radenovic, A.; Kuykendall, T.; Liphardt, J.; Yang, P. ZnO–Al₂O₃ and ZnO–TiO₂ core–shell nanowire dye-sensitized solar cells. *J. Phys. Chem. B* **2006**, *110*, 22652–22663. [[CrossRef](#)] [[PubMed](#)]
25. Dittrich, T.; Kieven, D.; Rusu, M.; Belaidi, A.; Tornow, J.; Schwarzburg, K.; Lux-Steiner, M. Current-voltage characteristics and transport mechanism of solar cells based on ZnO nanorods/In₂S₃/CuSCN. *Appl. Phys. Lett.* **2008**, *93*, 053113.
26. Kieven, D.; Dittrich, T.; Belaidi, A.; Tornow, J.; Schwarzburg, K.; Allsop, N.; Lux-Steiner, M. Effect of internal surface area on the performance of ZnO/In₂S₃/CuSCN solar cells with extremely thin absorber. *Appl. Phys. Lett.* **2008**, *92*, 153107.
27. Lévy-Clément, C.; Tena-Zaera, R.; Ryan, M.A.; Katty, A.; Hodes, G. CdSe-sensitized p-CuSCN/nanowire n-ZnO heterojunctions. *Adv. Mater.* **2005**, *17*, 1512–1515.
28. Liu, L.Q.; Hong, K.Q.; Liu, H.J.; Luo, Z.W.; Zhao, F.G.; Xu, M.X. Rapid growth of copper oxide nanorod arrays by a microwave heating approach. *Physica E* **2013**, *53*, 106–109. [[CrossRef](#)]
29. Liu, L.Q.; Ou, H.L.; Hong, K.Q.; Wang, L.X. Evidence of a strong electroneutral separation effect in ZnO@TiO₂ core/shell nanowires. *J. Alloys Compd.* **2018**, *749*, 217–220. [[CrossRef](#)]
30. Manthina, V.; Correa, B.J.P.; Liu, G.; Agrios, A.G. ZnO–TiO₂ nanocomposite films for high light harvesting efficiency and fast electron transport in dye-sensitized solar cells. *J. Phys. Chem. C* **2012**, *116*, 23864–23870. [[CrossRef](#)]
31. Park, K.; Zhang, Q.; Garcia, B.B.; Zhou, X.; Jeong, Y.H.; Cao, G. Effect of an ultrathin TiO₂ layer coated on submicrometer-sized ZnO nanocrystallite aggregates by atomic layer deposition on the performance of dye-sensitized solar cells. *Adv. Mater.* **2010**, *22*, 2329–2332. [[CrossRef](#)] [[PubMed](#)]
32. Palomares, E.; Clifford, J.N.; Haque, S.A.; Lutz, T.; Durrant, J.R. Slow charge recombination in dye-sensitized solar cells (DSSC) using Al₂O₃ coated nanoporous TiO₂ films. *Chem. Commun.* **2002**, *14*, 1464–1465. [[CrossRef](#)] [[PubMed](#)]

